JACS
JOURNAL OF THE AMERICAN CHEMICAL SOCIETY
Article
pubs.acs.org/JACS

Polarons, Bipolarons, and Side-By-Side Polarons in Reduction of Oligofluorenes

Lori Zaikowski,[†,‡] Parmeet Kaur,[†,‡] Claudia Gelfond,[‡] Elicia Selvaggio,[†,‡] Sadayuki Asaoka,[‡,⊥] Qin Wu,[§] Hung-Cheng Chen,[‡] Norihiko Takeda,[‡] Andrew R. Cook,[‡] Alex Yang,[‡] John Rosanelli,[‡] and John R. Miller*[,‡]

[†]Chemistry and Physics Department, Dowling College, Oakdale, NY

[‡]Chemistry Department and [§]Center for Functional Nanomaterials, Brookhaven National Laboratory, Upton, NY

Supporting Information

ABSTRACT: The nature of charge carriers in conjugated polymers was elucidated through optical spectroscopy following single- and multielectron reduction of 2,7-(9,9-dihexylfluorene) oligomers, F_n, n = 1−10, yielding spectra with the two bands typical of polarons upon single reduction. For short oligomers addition of a second electron gave a single band demonstrating the classic polaron−bipolaron transition. However, for long oligomers double reductions yielded spectra with two bands, better described as two polarons, possibly residing side-by-side in the F_n chains. The singly reduced anions do not appear to delocalize over the entire length of the longer conjugated systems; instead they are polarons occupying approximately four fluorene repeat units. The polarons of F_3 and F_4 display sharp absorption bands, but for longer oligomers the bands broaden, possibly due to fluctuations of the lengths of these unconfined polarons. DFT calculations with long-range-corrected functionals were fully consistent with the experiments describing polarons in anions, bipolarons in dianions of short oligomers, and side-by-side polarons in dianions of long oligomers, while results from standard functionals were not compatible with the experimental results. The computations found F_{10}^{2-}, for example, to be an open-shell singlet ($\langle S^2 \rangle \approx 1$), with electrons in two side-by-side orbitals, while dianions of shorter oligomers experienced a gradual transition to bipolarons with states of intermediate character at intermediate lengths. The energies and extinction coefficients of each anionic species were measured by ultraviolet−visible−near-infrared absorption spectroscopy with chemical reduction and pulse radiolysis. Reduction potentials determined from equilibria mirrored oxidation potentials reported by Chi and Wegner. Anions of oligomers four or more units in length contained vestigial neutral (VN) absorption bands that arise from neutral parts of the chain. Energies of the VN bands correspond to those of oligomers shorter by four units.

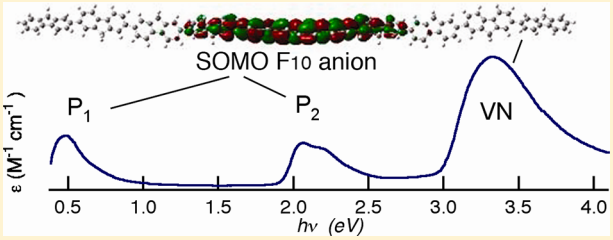

INTRODUCTION

Chemists have a long and ongoing quest to understand the nature of charge distribution, delocalization, and charge carriers in molecules. The horizons for delocalization broadened with the advent of conjugated polymers, recognized by the award of the Nobel Prize in Chemistry in 2000.[1] In these molecules the concept of a bare charge carrier does not fully account for experimental observations. Instead, charges and excitons in conjugated molecules are thought to form polarons: quasiparticles composed of charges and their accompanying polarization field. Polarons are the essential charge carriers in solar cells, sensors, and electronic devices, and their natures have impact on charge separation as well as transport. Experiments[2−17] and theory[13,17−22] on oligomers of definite lengths yield rich information about what polarons are like for both charges and excitons. To understand how these species participate in electron-transfer reactions, (both charge separation and recombination) and how they move within and between polymer chains, there remains a need for a deeper understanding of the nature of polarons. Experiments and theory described below seek answers to questions such as: (1) What are the delocalization lengths of electrons and singlet excitons? (2) When two electrons are introduced into an oligomer, how do they coexist in F_n chains of varied lengths? (3) What are the natures of the visible, NIR, and "neutral" absorption bands? (4) What are the energies (redox potentials) to inject electrons? (5) How well do computational methods describe the behaviors of the polarons, bipolarons, and related species? A central goal is to gain a better understanding, including a pictorial sense, of what polarons are like.

One-electron band theory predicts that single electrons or holes in conjugated systems will form polarons having two strong optical absorption bands, while bipolarons, two charges occupying the same region, have one strong band.[18−20] Experiments supported this paradigm, showing two bands (referred to as P_1 and P_2 for polarons) as well as possible formation of bipolarons with a single band at an energy

Received: February 14, 2012
Published: June 5, 2012

   dx.doi.org/10.1021/ja301494n | J. Am. Chem. Soc. 2012, 134, 10852−10863

between those of P_1 and P_2.[2−12] Molecular orbital calculations further supported these assignments.[23] In doubly reduced conjugated polymers electron spin resonance (ESR) measurements initially pointed to the dominance of bipolarons,[24] while later work implicated polarons.[25] In agreement with earlier work, van Haare and co-workers[14] found that injection of one and two positive charges gave polarons and bipolarons in 6 and 9-unit thiophene oligomers, but in a 12-unit oligomer injection of two charges gave bands more characteristic of two polarons residing in a single chain, a behavior that may model what occurs in polymers. Their results established the paradigm of two polarons in a single chain, but other processes such as disproportionation and formation of π-dimers complicated the data, preventing full conversion to species with two polarons/chain.

Polyfluorenes and their copolymers find use in light-emitting diodes (LEDs) and organic photovoltaics.[26,27] Oligofluorenes provide conduits for "wire-like" transfer of charges,[28−31] and fast transport of excitons.[32,33] Electrons and holes transport rapidly along polyfluorene chains,[34−36] and high charge and exciton mobilities are observed in their films.[37−39] Polarons, either charged or excitonic, are the carriers in nearly all of these processes. Oligofluorenes can also produce blue lasers.[40−43]

The present study examines the F_1−F_{10} oligo-2,7-(9,9-dihexylfluorene) series (Figure 1) to understand more deeply

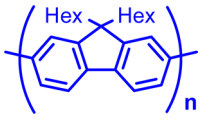

Figure 1. Structure of oligofluorenes, F_n, n = 1−10.

the phenomenon of "two polarons in a single chain." The results show clearly the formation of polarons, the effects of delocalization, the formation of bipolarons in short oligomers, and the evolution to pairs of polarons in longer ones. The results also find this transition not to be abrupt, but to create states having character that appears to be intermediate between bipolarons and two side-by-side polarons. Additional information comes from portions of the F_n chains that remain neutral.

Fratilou[17] measured optical spectra and performed DFT calculations for singly reduced or oxidized F_n, n = 1−5. The present results to n = 10 include polarons not confined by the length of the chain in which they are trapped. Unconfined polarons are expected to present a particular challenge to DFT methods, which tend to overestimate delocalization due to self-interaction error.[44−46] The experimental results described below are therefore an excellent test of DFT methods including recently developed long-range-corrected functionals,[47−50,54] so predictions of both standard and long-range-corrected functionals are compared with the experimental results.

RESULTS

Absorption spectra of the neutral oligofluorenes (F_n) (Figure 2) indicate that as length increases up to F_5, the maxima of the spectra (E_{max}) shift to lower energies, but from F_5 to F_{10} E_{max} changes little although the extinction coefficient increases approximately linearly with length. A similar pattern is observed in the fluorescence emission spectra (Figure 3). These data follow trends observed by Jo,[51] who studied lengths to F_7.

Chemical Reduction with Na, NaK, and NaBip. The oligofluorenes are reduced by sodium or similar agents, F_n + Na

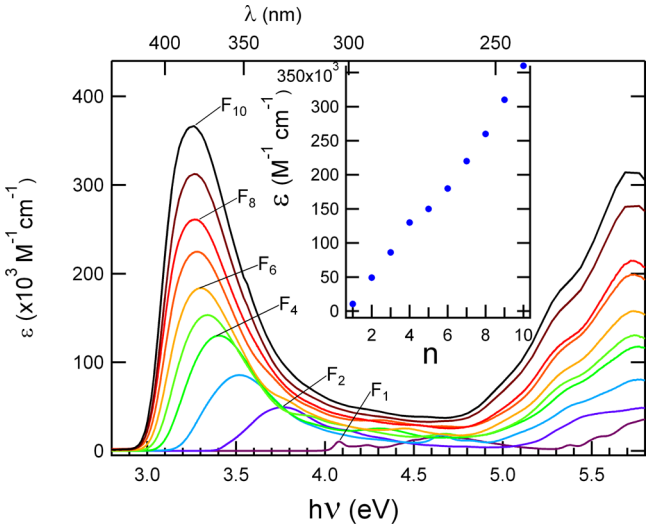

Figure 2. Optical absorption spectra of oligofluorenes, F_1−F_{10} neutrals in THF. The inset plots the extinction coefficient (ε) at the maximum vs the number of repeat units.

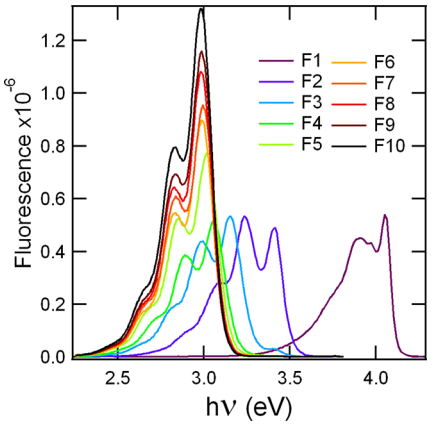

Figure 3. Fluorescence emission spectra of F_1−F_{10} neutrals. Concentrations were 2 × 10^{-6} M in THF excited at 300 nm except F_1, which was excited at 265 nm. λ_{max} in nm: F_1 = 306, 317; F_2 = 363, 383; F_3 = 393, 415; F_4 = 406, 429; F_5 = 411, 435; F_6 and F_7 = 414, 438; F_8−F_{10} = 415, 438. The spectra are not normalized; intensities increase for F_5−F_{10} due to the increase in absorption at the excitation wavelengths in the 1 cm^2 cells.

→ $F_n^{-\bullet}$ + Na^+. A great simplification comes from the stability of the anions, which show no indication of losses that come from side reactions, such as π-dimerization. Figure 4 shows optical absorption spectra for single and double reduction of oligomers F_n, n = 2−10. These results are principally from titrations with sodium biphenyl (NaBip), but also utilized data from two other methods: reduction by sodium mirrors (Na), or reduction by sodium−potassium alloy (NaK) followed by back-titration (see Experimental Section). Where more than one method was employed the results were consistent. The spectra are consistent with those reported by Fratiloiu[17] for singly reduced F_n, n = 2−5, but the present experiments obtain both single and double reductions, a wider wavelength range enabling more complete observation of the near-infrared bands of longer oligomers, observation of the region of neutral absorption and enhanced signal/noise.

For short oligomers the spectra change rapidly with length, n, and with the number of electrons added. In most cases the

dx.doi.org/10.1021/ja301494n | J. Am. Chem. Soc. 2012, 134, 10852−10863

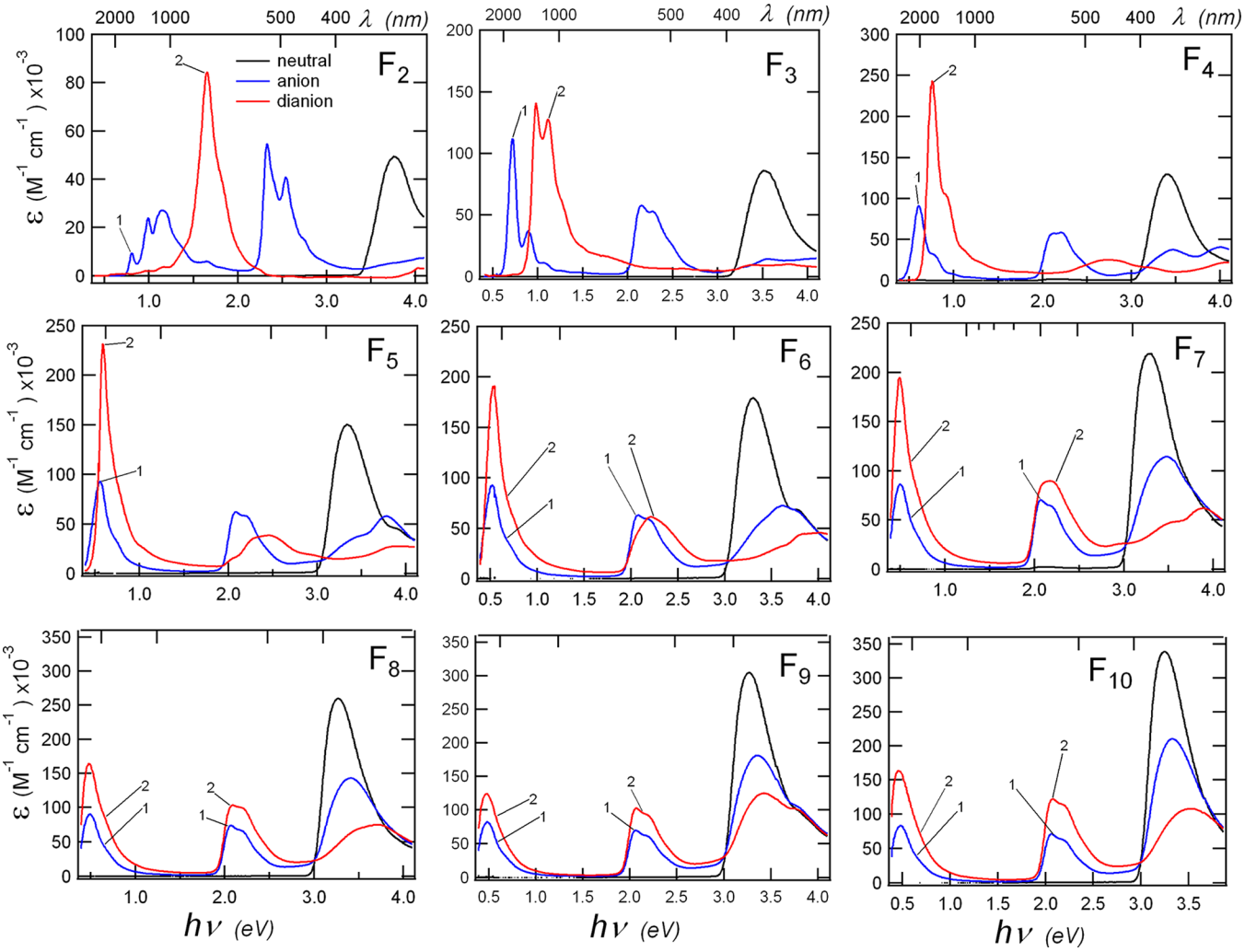

Figure 4. Optical spectra of oligofluorenes, F_n, $n = 2-10$. Labels on some spectra indentify the F_n with one or two added electrons per F_n molecule.

shapes, positions and extinction coefficients of anion bands were insensitive to the method of reduction. For anions five units or longer the positions of the NIR P_1 polaron bands were identical within 1.5% for the NaBip titrations, the Na mirror reductions, and NaK reductions. For $F_4^{-\bullet}$ the E_{max} of the P_1 band increased by 0.037 eV (6% of E_{max}) when formed by NaK reduction, probably due to ion pairing with K^+. The visible P_2 band shifted blue by only 0.4%. A corollary of the observations is that $F_4^{-\bullet}$ is ion-paired, at least with K^+, but $F_5^{-\bullet}$ and anions of longer oligomers are either free ions or their spectra are insensitive to ion-pairing. This conclusion is further supported by the absence of spectral shifts during reduction of the longer oligomers. Dissociation constants reported by Slates and Szwarc for Na^+ paired with radical anions in THF were 0.15 and 1.15 × 10^{-6} M for the two-ring aryls naphthalene and biphenyl, but increased to 1.5 and 2.3 × 10^{-5} M for four and five ring compounds.[52] If for $F_5^{-\bullet}$ with ten rings, K_d is at least this large, then ~half or more of the $F_5^{-\bullet}$ ions would be free of their Na^+ counterions under our conditions. Similarly addition of the 222 cryptand in reduction of F_7 with NaBip changed E_{max} of the anion P_1 band by <0.5%, which is within experimental uncertainty. The −2 charge of dianions would approximately double the free energies for ion-pairing relative to those for the corresponding anions. Therefore if $K_{diss}(F_5^{-\bullet},Na^+)$ is ~10^{-4} then for the dianion $K_{diss}(F_5^{-2},Na^+)$ would be ~10^{-8}, leading to the prediction that dianions will be almost completely paired with a counterion under the present conditions. The NIR band of F_7^{-2} formed by NaK reduction was shifted blue by 100 nm relative to dianions formed by Na or NaBip reduction, showing that the dianions are ion-paired by K^+. The visible band of F_7^{-2} was shifted little by K^+, indicating that the energy of visible transition is not sensitive to ion-pairing..

Spectra of anions of longer oligomers have prominent absorption bands in the region where the neutral had absorbed. The behavior of these bands, discussed below, suggests that they are vestiges of the neutral bands. Similar bands are seen in the neutral region when the anions are created by reaction with solvated electrons, which eliminates ion-pairing (Figure S3, Supporting Information [SI]). The spectrum of $F_1^{-\bullet}$ is shown in Figure S4, SI.

Figure 5 replots the spectra of anions and dianions so they may be compared. Figure S1 [SI] highlights the contrasting behavior of short and long oligomers upon single and double reduction. $F_3^{-\bullet}$ and $F_{10}^{-\bullet}$ both display classic polaron spectra, and F_3^{-2} is a classic bipolaron. F_{10}^{-2} instead displays a spectrum of side-by-side polarons. Figure S2 [SI] compares ions with the same number of electrons per repeat unit. For several ions resolved side-bands appear which may arise from coupling of the transitions to molecular vibrations. Energy differences are collected in Table S1 [SI].

dx.doi.org/10.1021/ja301494n | J. Am. Chem. Soc. 2012, 134, 10852−10863

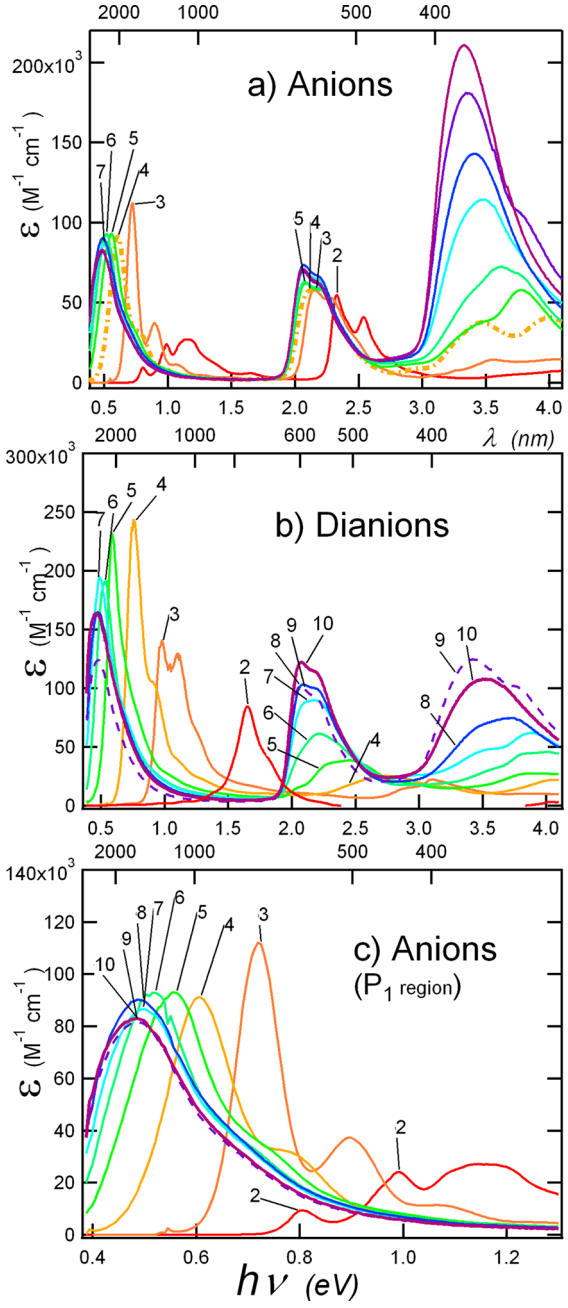

Figure 5. Comparison of optical spectra of all (a) anions, (b) dianions, and (c) an expanded view of low-energy spectra of anions. The spectra are all from Figure 4. Labels indicate lengths, *n*.

Computed and Observed Polaron Transition Energies and Orbitals. Table 1 presents computed lowest transition energies for oligofluorene neutrals and anions. Unrestricted DFT was used for all calculations on anions and dianions. Those of the anions are also plotted in Figure 6 vs oligomer length as $1/n$, in comparison with observed P_1 and P_2 transitions based on data in Figure 4. Experimentally, energies of the P_2 transitions are relatively insensitive to *n*, as noted previously,[53] changing only by 12% from $n = 2-10$. The energies of the P_1 transitions change by a factor of 2 over the same length. They change rapidly with n at short lengths, but become almost constant for $n > 5$. B3LYP does a good job predicting neutral transitions, but it severely underestimates the P_1 transitions in long anions. Moreover, transitions computed

Table 1. Calculated First Transition Energy (in eV) for Both Neutral and Anions of Selected Oligofluorenes[a]

n	F_n/ expt	F_n/ B3LYP	F_n/ ωPBE	F_n^-/ expt	F_n^-/ B3LYP	F_n^-/ ωPBE
2	3.48	3.7131	3.6272	0.987	1.1736	1.0903
4	3.15	3.2372	3.2231	0.608	0.6433	0.6496
6	3.08	3.1228	3.1276	0.521	0.4249	0.5418
8	3.07	3.0781	3.0886	0.492	0.3166	0.5269
10	3.07	3.0575	3.0709	0.483	0.2545	0.5249

[a]TDDFT calculations were performed at the geometry optimized in the ground state with the same functional. All calculations use the standard basis set 6-31G* and the PCM model for solvation in THF. For ωPBE calculations $\omega = 0.1$ bohr^{-1}.

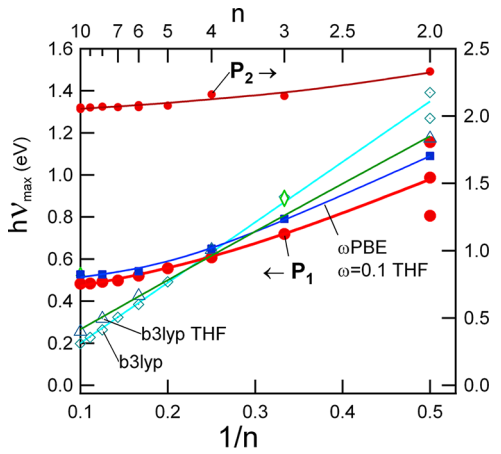

Figure 6. Energies of the two principal transitions, P_1 (left axis) and P_2 (right axis) in $F_n^{-\bullet}$ anions vs reciprocal length. The energies of the observed P_1 transitions are compared with energies computed by unrestricted TDDFT with B3LYP/6-31G* (in vacuum and in THF), and ωPBE/6-31G* ($\omega = 0.1$) in THF. Calculations in THF used the PCM solvation model.

by B3LYP change almost linearly with $1/n$, reflecting the almost complete delocalization over even the longest oligomers. This remains true when the $F_n^{-\bullet}$ anions were optimized in and the TD calculations carried out in a PCM reaction field modeling solvation in THF. This contrasts to the near constancy of the observed transitions for $n > 5$. Overdelocalization, a result of self-interaction error, typical of standard functionals, produces the decreased transition energies.[44] Results with the long-range-corrected ωPBE functional[54] ($\omega = 0.1$ bohr^{-1}) in THF better follow the observed experimental pattern. In vacuum (no reaction field) ωB97X-D and ωPBE ($\omega = 0.2$ bohr^{-1}) give similar results, but in further contrast to B3LYP, the ωPBE results depend strongly on ω in the reaction field. For $\omega = 0.2$ bohr^{-1} in THF the polarons are more confined and the computed transition energies almost doubled.

These results suggest that the ω value is a critical parameter in predicting the polaron size. We have adjusted ω to reproduce the experimental P_1 transitions in the anions. While this approach parametrizes computations to experiment, it should nevertheless be considered a success for the range-separated functionals that a single parameter can capture the trend in a series of molecules. Furthermore, the same ω value (0.1 bohr^{-1}) seems to work equally well for neutral molecules as shown in Table 1. We are currently investigating the transferability of this parameter to different systems.

dx.doi.org/10.1021/ja301494n | J. Am. Chem. Soc. 2012, 134, 10852−10863

The inclusion of an Na^+ ion was found to increase the energy of the computed P_1 transition relative to transitions computed in vacuum. This finding agrees with computations by Zamoshchik and Zade on oligothiophene cations.[13,55] On the other hand because the $F_n^{-\bullet}$ anions produced here are principally free of ion-pairing, or the spectra are not affected (see the section on Chemical reduction, above), the most appropriate calculations include a solvent model but not a counterion.

Figure 7 displays orbitals for F_{10} anions and dianions comparing results computed by unrestricted B3LYP with those

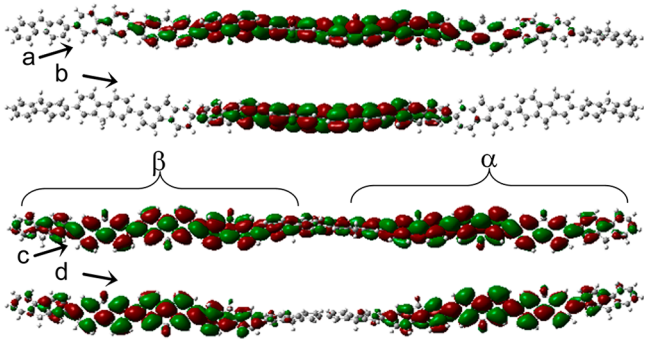

Figure 7. Orbitals computed for ions of F_{10} with 6-31G* and the PCM solvation model for THF. (a) The SOMO of $F_{10}^{-\bullet}$ computed with uB3LYP, which delocalizes electrons over much of the oligomer. (b) The SOMO of $F_{10}^{-\bullet}$ computed by the long-range-corrected unrestricted functional uωPBE (ω = 0.1), which delocalizes electrons over ~4.5 repeat units. (c) The partly overlapping HOMOs of spin α and β of the open-shell singlet F_{10}^{-2} computed with uB3LYP and (d) with ωPBE (ω = 0.1). All surfaces have the isovalue of 0.01.

computed by ωPBE (ω = 0.1), both using 6-31G* and the PCM solvation model for THF. While the B3LYP SOMO of $F_{10}^{-\bullet}$ is more delocalized than the observed spectra indicate, the ωPBE/6-31G* SOMO is in good accord with the experiments that point to a polaron length of ~4.3 repeat units. For the F_{10}^{-2} dianion both B3LYP and ωPBE (ω = 0.1) functionals predict α and β HOMO's to be side-by-side polarons, also in agreement with experiment. B3LYP predicts substantial overlap of the two orbitals, while ωPBE predicts some neutral space between them, more in accord with the observed VN band of F_{10}^{-2}. More realistic calculations for F_{10}^{-2} might include one positive counterion which would reduce Coulomb repulsion, but we have found these computations to be challenging for dianions.

F_{10}^{2-} in Figure 7 was computed using unrestricted determinants while requiring the spin multiplicity to be 1. It is an open-shell singlet with $\langle S^2\rangle$ = 1.0633, which means the two extra electrons occupy two separate orbitals having little overlap. The next section describes the utility of $\langle S^2\rangle$ in deciding between bipolarons and side-by-side polarons. Further evidence can be found in TDDFT spectra. The calculated first peak for F_{10}^{2-} is at 0.5549 eV with an oscillator strength of 3.22. This strength is almost twice that of the P_1 transition computed for F_{10}^{-}, and the transition energy differs only by 0.12 eV. This computed result is in excellent agreement with experiment (see Figure 4, last panel) and with the notion that F_{10}^{-2} comprises two side-by-side polarons that perturb each other only moderately.

Calculations on dianions of short oligomers produced results that changed with length, n. For F_1^{-2} and F_2^{-2} the stable solutions are true singlets with $\langle S^2\rangle$ = 0, which means the two extra electrons occupy the same orbital: F_1^{-2} and F_2^{-2} are computed to be pure bipolarons. This is also seen in Figure 8

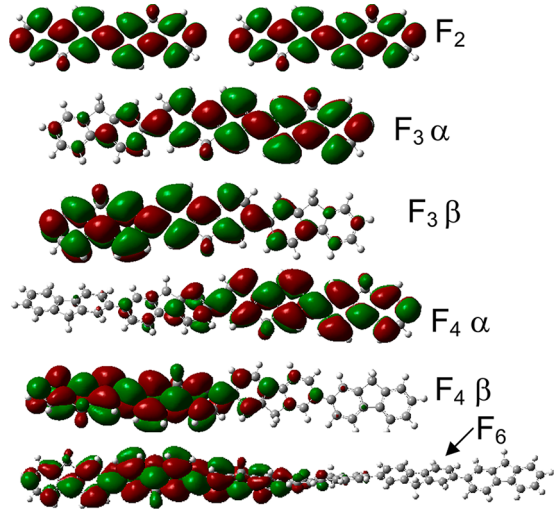

Figure 8. α and β HOMOs for dianions F_2^{-2}, F_3^{-2}, F_4^{-2}, and F_6^{-2}, computed by uωPBE/6-31G* (ω = 0.1) with PCM solvation in THF showing the transition from principally bipolaron character in F_2^{-2} to principally side-by-side polarons in F_4^{-2} and F_6^{-2}. The β HOMO of F_6^{-2} (not shown) is a mirror image of the α.

which shows that the α and β HOMOs of F_2^{-2} are indistinguishable. F_3^{-2} with $\langle S^2\rangle$ = 0.69 is a mixture of bipolaron and side-by-side polaron character, as is also seen from plots in Figure 8. F_4^{-2} ($\langle S^2\rangle \geq 0.95$) and F_6^{-2} ($\langle S^2\rangle \geq 1.01$,) have almost completed the transition to separate polarons. While F_4^{-2} and F_6^{-2} (orbitals shown in Figure 8) appear to comprise two polarons, the two are not each 4.3 units long, but both are compressed and partly overlap to fit into the F_4 and F_6 chains. The calculations were constrained to be singlets; triplets had higher energies. The solvation model in these calculations make them more realistic, but they do not include counterions, almost certainly paired with dianions in the experiments. The counterions probably reduce Coulombic repulsion, making bipolaron formation somewhat more favorable.

$\langle S^2\rangle$ as a Diagnostic for Bipolarons vs Side-by-Side Polarons. In an unrestricted calculation of the singlet state, the spatial orbitals of α and β spins are allowed to be different in order to lower the ground-state energy. When there is a difference, the single determinant formed from these orbitals is not an eigenfunction of the total spin operator S^2, and we see nonzero S^2 values even for singlet states. Mathematically, the S^2 value is calculated directly from the spatial overlap of spin orbitals (eq 2.271, p 107 in ref 56). For the dianions we are studying here, we may make a reasonable assumption that all orbitals for α and β spins have identical spatial components except for the HOMOs, i.e. the orbitals occupied by the two additional electrons. If we denote the overlap integral between these two orbitals as s, it can be shown that the S^2 value is equal to $1-s$. Electron repulsion tends to push these two orbitals toward opposite ends of a chain molecule. As the chain length increases, these orbitals overlap less and less until they become disjoint,[57] at which point it is suggested side-by-side polarons are formed.[21,58] In this process, s decreases from 1 to 0, and S^2 increases from 0 to 1. This correlation between the S^2 value and

dx.doi.org/10.1021/ja301494n | J. Am. Chem. Soc. 2012, 134, 10852−10863

Table 2. Reduction Potentials $E^{0/-}$ vs $Fc^{+/0}$ for Oligofluorenes, K_{eq} and k_{fwd} with Comparisons to the Corresponding Potentials for Oxidation

	reaction	k_{fwd} (10^9 M^{-1} s^{-1})	[A][a]	K_{eq}[b]	$E^0(F_n)^{0/-}$[c]	$\Delta E^{0/-}$ mV[e]	$E^0(F_n)^{+/0}$[d]	$\Delta E^{0+/0}$ mV[e,f]	ΔE^0_n mV vs F_7[g]
F_1	$F_1^{-\bullet}$ + Phen	2.0	0.2−20	700	−3.084	−290	(1.17)[f]		483
F_2	$Phen^{-\bullet}$ + F_2	0.79	0.033−1.67	129.5	−2.793	−113	0.88	110	187
F_3	$F_2^{-\bullet}$ + F_3	2.1	0.025−0.13	86.4	−2.680	−50	0.77	40	75
F_4	$F_3^{-\bullet}$ + F_4	1.4	0.025−0.13	7.13	−2.630		0.73	50	30

[a]Concentration range of the acceptor, Phen, F_2, F_3, and F_4; concentration of the donor, F_1, Phen, F_2, and F_3 were 100 mM, 10 mM, 5 mM, and 0.5 mM, respectively. [b]Equilibrium constant for the reaction (uncertainty ±15%) was determined from five kinetic traces with different concentrations of acceptor. [c]Redox potentials (V vs Fc) from charge-transfer equilibrium constants with phenanthrene using $E^0(Phen^{0/-}) = -2.917$ V vs $Fc^{+/0}$ from $E^{0/-}$ for anthracene[60] vs $Fc^{+/0}$ and the difference between reduction potentials for anthracene and phenanthrene.[61] [d]Potentials for oxidation of oligofluorenes from Chi and Wegner[16] vs $Fc^{+/0}$. For n = 5, 6, and 7 their potentials were 0.68, 0.70, and 0.70, respectively. [e]Difference between E^0 and that for the next longer oligomer (mV). [f]Estimated from the potential[16] for F_2 and the difference, determined here, between potentials for reduction of F_2 and F_1, relying on the assumption that potentials for oxidation and reduction mirror each other. [g]Difference in the potential $E^0(F_n)^{+/0}$ or $-E^0(F_n)^{0/-}$ relative to the potential[16] for a long chain, n = 7, a length at which polarons should not be confined by the length of the chain. These differences, which are similar for anions and cations, will be interpreted as polaron compression energies (see Discussion). The compression energy is nearly constant (−20, 0, 0 meV) for n = 5−7 based on Chi's results (see ref 16 or footnote *d* of this table).

the contribution of polaron pair configurations has been observed before.[21] Here we use it as an approximate but convenient tool for describing the bipolaron to side-by-side polarons transitions.

Determination of Redox Potentials for Oligofluorenes (F_n, n = 1−4). Table 2 reports reduction potentials ($E^{0/-}$) for F_n (n = 1−4) and their comparison to the corresponding potentials for cations determination by Chi and Wegner.[16] Chi did not report potentials for creation of anions, which were too unstable to permit measurements.[16] Therefore, the potentials were measured by determination of equilibrium constants for bimolecular electron transfer using pulse radiolysis at Brookhaven's Laser Electron Accelerator Facility (LEAF). Measurements were in THF containing electrolyte. The largest drop in potential, from F_1 to F_2, was measured in two steps. Figure 9 shows one of the sets of traces used to determine the

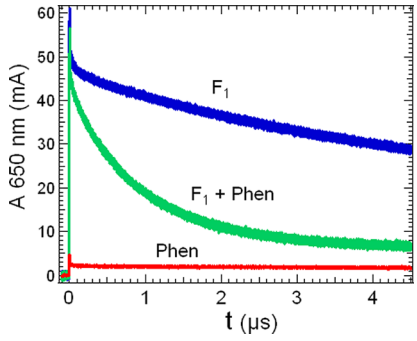

Figure 9. Kinetic traces at the 650 nm λ_{max} of $F_1^{-\bullet}$ from pulse radiolysis of (top to bottom) 100 mM F_1, 100 mM F_1 + 0.8 mM phenanthrene (Phen), and 48 mM Phen solutions in THF all containing 10 mM NaBPh4.

first of these steps, electron transfer from $F_1^{-\bullet}$ to phenanthrene (Phen). From Figure 9 and similar data, K_{eq} = 700 and k_{fwd} = 1.97 × 10^9 M^{-1} s^{-1} for $F_1^{-\bullet}$ + Phen ⇌ F_1 + $Phen^{-\bullet}$. The reduction potential of phenanthrene provided reference to electrochemical measurements. The methods are similar to those described previously.[36,59] The results in Table 2 confirm the suggestion of Chi[16] that the spacings between potentials for reduction of F_n would mirror those for the corresponding oxidations to cations.

In titrations with sodium biphenyl the growth of F_2^{-2} occurred simultaneously with growth of $biphenyl^{-\bullet}$, enabling determination of the potential for reduction of $F_2^{-\bullet}$ to F_2^{-2} from the equilibrium constant for the reaction $biphenyl^{-\bullet}$ + $F_n^{-\bullet}$ ⇌ biphenyl + F_n^{-2}. This redox potential and the one for F_3 were $E^0(F_2^{-1/-2}) = -2.96$ and $E^0(F_3^{-1/-2}) = -2.80$ vs $Fc^{+/0}$.

DISCUSSION

The discussion will examine the results in terms of known concepts and seek to relate phenomena such as the broadening of spectra for long oligomers, vestigial neutral bands, redox potentials, and computed results in an attempt to assemble a simple, pictorial view of the natures of the charges residing in the oligomers. For the spectra presented in the Results section it will be advantageous to make comparisons not easily done in Figure 4; thus, graphs of the spectra will be assembled in different ways in Supporting Information, and in one case in this Discussion.

Spectra of F_n Neutrals: Excitonic Polarons. The optical absorption spectra of the neutral oligofluorenes change rapidly with length for small n, and more slowly at large n, but a spectral shift is still noticeable between F_9 and F_{10}. The findings and interpretations are fully compatible with those of Chi, Im and Wegner,[15] who examined fluorene oligomers up to seven units. The fluorescence spectra behave differently. Like the absorption spectra they change rapidly from F_1 through F_4, but the spectra in Figure 3, like those of Chi,[15] are almost indistinguishable from n = 5−10. This suggests that the exciton is delocalized over five monomer units, but does not spread further. The different length-dependence of absorption and fluorescence can be understood on the basis of the effects of geometrical relaxation of excited states in conjugated systems discussed by Jansson.[22] The energies of absorption transitions depend on both the ground- and excited-state wave functions. The gradual shifts of absorption spectra for $n \geq 5$ can be understood in terms of unrelaxed, Franck−Condon excited-state wave functions formed vertically in the transition, which may have lengths up to 10 or more units. The fluorescence involves the relaxed exciton, which we conclude has a length of 5 units.

Polaron Delocalization Lengths in Anions. The maxima of the P_1 and to a lesser extent those of the P_2 transitions of anions in Figure 6 change rapidly with oligomer length, n, for n = 2−4, as do the shapes of the spectra of anions in Figure 4. The changes are modest for n = 4−7, and change little for n = 7−10. This evolution of oligomer spectra is consistent with the conclusion by Takeda[59] that electrons injected into polyfluor-

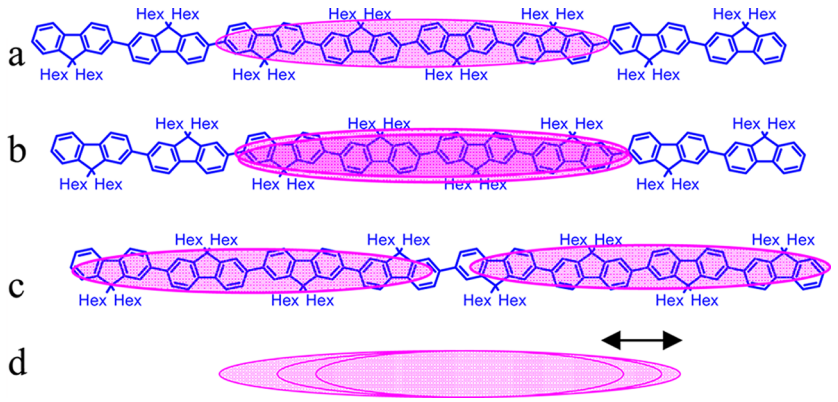

Figure 10. Simplified picture of charges in F_8. (a) A single electron as a polaron occupying four repeat units, (b) a bipolaron in which two charges occupy the same region, (c) two side-by-side polarons, (d) fluctuations in the length of a polaron, possibly due to fluctuations of dihedrals (see below).

enes delocalize over n_{deloc} = 4.5 ± 0.5 repeat units. Pertinent features of the data are the following: (1) The large shifts in the absorption spectra for F_n anions, n = 2−4 demand a delocalization length >3 repeat units. The spectra are invariant within experimental uncertainty for n = 7−10, so $n_{deloc} \leq 7$. (2) For n = 4−7 modest changes are seen in the peak energies of the P_1 bands and in their (extrapolated) onsets. These changes could be interpreted to indicate that the polaron spreads over more than 4.5 units. However, as with the neutral molecules,[22] absorption spectra of anions reflect the differences between their relaxed ground states and unrelaxed excited states. The observed changes could reflect solely differences in the spread of the unrelaxed excited states, so they are not decisive in determining delocalization lengths. (3) The absorption spectra show sharp bands with resolved vibrational structure for n = 2−3 that are broader for n = 4 and that reach a larger, constant width for n = 5−10. A possible reason for this broadening is discussed below. The constant width, as well as position, for $n \geq 5$ thus implies that the length of the polaron becomes constant for $n \geq 5$. (4) Redox potentials (Table 2) solely depend on properties of the ground state. The potential changes by 290 mV from F_1 to F_2, 113 mV from F_2 to F_3, and only 50 mV from F_3 to F_4. The small stabilization of 50 meV of $F_4^{-\bullet}$ relative to $F_3^{-\bullet}$, only twice kT at room temperature, is close to values that might be expected from entropic stabilization if the polaron does not fill the full length of the oligomer. We therefore conclude that the redox potentials imply that $n_{deloc} \geq 4$. Where observable, the splittings (Table S1 [SI]) of peaks, possibly due to vibrations, decrease for P_2 bands of anions, and become approximately constant $n \geq 4$. The results from spectral positions and widths and redox potentials, taken together, thus lead to $4 \leq n_{deloc} \leq 5$, in accord with the earlier report of Takeda[59] that n_{deloc} = 4.5 ± 0.5. Information from "vestigial neutral" bands, discussed below, will favor the lower part of this range, n_{deloc} = 4.3 ± 0.5.

Transitions in Dianions. Spectra of dianions display the P_1 and P_2−like structure of (side-by-side) polarons for lengths longer than ∼7 repeat units. But the NIR band develops over a range of lengths and still changes from F_9^{-2} to F_{10}^{-2}, at which point the spectrum closely resembles two separate polarons as noted in Figure S1 (SI). This is consistent with the idea that two side-by-side polarons require ∼twice the 4.3 unit delocalization length of polarons. The structure of side-by-side polarons in e.g. F_{10}^{-2} is not known, but a candidate is described by the computed orbitals in Figure 8, the pairs of polarons separated by a neutral space.

Redox Potentials and Polaron Compression. The redox potentials of Chi and Wegner[16] and those determined here have a nearly identical dependence on oligomer length, n. This length dependence, shown in Table 2 as ΔE^0_n can be interpreted in a simple way. We propose that ΔE^0_n provides an approximate estimate for the energy required to compress a polaron to length n. This "polaron compression energy" is 30 meV, just barely larger than kT, for F_4, and rises to 483 meV for F_1. It is close to zero for $n > 4$ (see Table 2 and its footnotes). One of the uses of ΔE^0_n is to estimate the minimum energy for formation of side-by-side polarons. For example the energy of a side-by-side in F_6^{-2} would require at least $2\Delta E^0_3$ = 150 meV; additional contributions arise from other sources such as Coulombic repulsion and differences in solvation energies. The "compression" contribution, $2\Delta E^0_{n/2}$, is 966, 374, 150, and 60 meV respectively in F_2^{-2}, F_4^{-2}, F_6^{-2}, and F_8^{-2}. These estimated energy contributions to formation of side-by-side polarons are larger than the differences between first and second redox potentials reported here for F_2, or the corresponding differences for cations.[16] Doubly charged short oligomers are therefore predicted to be bipolarons, while longer ones are likely to form side-by-side polarons in agreement with the spectra in Figure 4.

Disproportionation of Anions. Upon formation of a radical anion the spectrum due to the neutral is normally completely eliminated.[62] In Figure 4 the band of F_2 neutral is completely absent, within experimental uncertainty, in the spectra of $F_2^{-\bullet}$, when the electrons added per molecule, m, is 1.0. For F_3 at m = 1.0, ∼3% of the neutral remains and ∼3% is converted to dianion; a total of 6 ± 2% of $F_3^{-\bullet}$ ions have converted to neutrals and dianions in a disproportionation equilibrium:

$$2F_n^{-\bullet} \rightleftharpoons F_n^{-2} + F_n \quad (1)$$

$$\Delta G^\circ_{disp} = E^0(F_n^{-1/-2}) - E^0(F_n^{0/-1}) \quad (2)$$

In anions of longer oligomers total disproportionation was larger: 12 ± 4% in $F_4^{-\bullet}$, 15 ± 5% in $F_5^{-\bullet}$, and 20 ± 5% in $F_6^{-\bullet}$, yielding K_{disp} = 6, 9, and 13 × 10^{-3}, respectively. Equation 2, written particularly for disproportionation of anions, applies for other redox states including oxidation. It may be used to estimate disproportionation of $F_n^{+\bullet}$ cations, dications, or trications from the redox potentials of Chi and Wegner.[16]

dx.doi.org/10.1021/ja301494n | J. Am. Chem. Soc. 2012, 134, 10852−10863

Their potentials lead to disproportionation of 0.03% ($F_2^{+\bullet}$), 0.2% ($F_3^{+\bullet}$), 1.4% ($F_4^{+\bullet}$), 4% ($F_5^{+\bullet}$), 8% ($F_6^{+\bullet}$), and 16% ($F_7^{+\bullet}$). Compared to $F_n^{-\bullet}$ anions reported here, the degree of disproportionation of $F_n^{+\bullet}$ cations is less by a factor of ∼2 but follows a similar dependence on oligomer length. The redox potentials of Chi and Wegner[16] predict that di- and trications will also disproportionate to an extent slightly smaller than for monocations. In the present results ∼20% disproportionation was noticeable for trianions of F_5 and F_6, but it was not evident in other cases, often because spectra were not sufficiently distinct. For anions of F_7−F_{10} disproportionation was almost certainly present, but the amount could only be roughly estimated to be ∼30% because large "vestigial" neutral bands discussed below interfered with its determination.

Vestigial Neutral Bands Remaining in Anions. At m = 1.0 electrons per molecule the spectra of $F_4^{-\bullet}$−$F_{10}^{-\bullet}$ in Figure 4 contain absorption bands resembling the absorption bands of the neutrals. Here we consider the interpretation, depicted in Figure 10, that these bands are due to absorption by neutral segments of the $F_n^{-\bullet}$ molecules. For example in $F_8^{-\bullet}$ if the negative polaron occupies 4.3 fluorene units, then 3.7 units remain neutral and might be expected to exhibit absorption similar to a neutral oligofluorene of that length.

From the spectra in Figure 4 one can see that these "vestigial neutral" (VN) bands in $F_n^{-\bullet}$ anions are shifted to higher energy and have reduced intensity compared to the spectra of the completely neutral F_n molecules of the same length. Figure 11

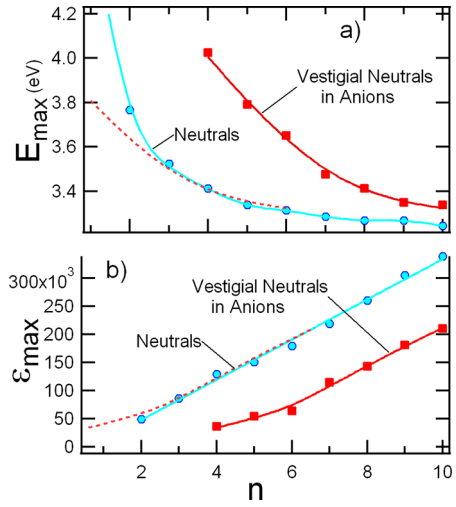

Figure 11. (a) Energies of absorption maxima, E_{max}, and (b) extinction coefficients, ε_{max}, for F_n neutrals and vestigial neutral (VN) bands in anions, $F_n^{-\bullet}$, plotted vs oligomer length, n. The dashed lines are the curves for VN bands shifted by Δn = −4.0 (for E_{max}) and Δn = −3.4 ± 0.3 repeat units (for ε_{max}).

compares the peak energies, E_{max}, and extinction coefficients at the peaks, ε_{max}, for VN bands of $F_n^{-\bullet}$ with those of the neutral molecules, F_n. The plots of E_{max} and ε_{max} of the VN bands are parallel to those of neutral bands for $n \geq 3$ but shifted by Δn = −4.0 ± 0.5 and −3.4 ± 0.3 units, as illustrated by the dashed curves. The shapes of the VN bands are also similar, although not identical to those of shorter neutrals. The VN band of $F_{10}^{-\bullet}$, for example, is similar to the neutral spectra of F_5 or F_6. A plausible interpretation of these results is that the VN bands are transitions of neutral portions of the oligomeric chains, but shorter because they include parts not covered by the polaron.

The presence of a negative polaron apparently shortens the effective length of the neutral portion by ∼3.4−4.0 repeat units, providing another estimate for the length of the polaron. Figure 10 gives a useful pictorial description but is probably oversimplified. The figure could be taken to suggest a sharp interface between the polaronic and neutral portions of the oligomeric chain, while some interpenetration of wave functions may be likely. A polaron immediately adjacent to a neutral segment, and possibly interpenetrating with it, may alter the properties of that segment. A theory describing absorption of neutrals adjacent to polarons might clarify the picture, but we are not aware of availability of such a theory.

The spectra of dianions of longer oligomers in Figure 4 also contain what appear to be VN bands that show these characteristics: (1) The VN neutral region bands in dianions are smaller and appear at higher energies than the VN bands of anions. (2) They generally become more intense for longer oligomers. (3) Most appear to have at least two poorly resolved peaks. Neither of these is at the energy of the neutral, but one is at or close to the energy of the VN band of the anion. While the natures of these bands are not clear, their double-peaked spectra in the neutral region may be due to a VN band of the dianion, and a lower-energy VN band of anions formed by disproportionation. The two have approximately equal intensities at m = 2.0 electrons/molecule because most of the molecules are present as dianions, but the VN bands of the anions have much larger extinction coefficients. Figure S6 [SI] displays spectra of three dianions corrected for VN bands of anions to estimate the VN bands of the dianions. The fact that the VN bands of dianions are weaker (smaller extinction coefficients) and occur at higher energies than those in anions is consistent with the idea that the dianions contain two polarons, but there are quantitative differences noted with Figure S6 [SI]. It could also be consistent with the idea that the dianions contain bipolarons if the length of a bipolaron is substantially longer than the length of a polaron.

Disproportionation and Vestigal Neutral Bands. Both cause neutral-like bands to appear in spectra of anions, but they arise in different ways and behave differently. Figure S7 in SI shows an example of this contrasting behavior in the titration of F_5. Disproportionation produces completely neutral F_5 molecules, even when there is 1.0 e^- per F_5, so that it gives a peak exactly at E_{max} of the neutral. The vestigial neutral band appears at a distinctly shorter wavelength. And as seen in Figure S7 [SI] the VN band rises, reaches maximum and decreases in exact proportion to anions; it and the anion bands decrease almost linearly with added electrons from m = 1.0 to m = 2.0 e^-/molecule. The neutral bands from disproportionation decrease more rapidly as electrons are added, falling by more than a factor of 2 from m = 1.0 to m = 1.2, as expected for $K_{disp} = 9 \times 10^{-3}$. Over this range the VN band decreases only by 20%.

Bipolarons vs Side-By-Side Polarons. It was noted above (see Figure S1 [SI]) that dianions of F_2 and F_3 conform to the classic description[23] of bipolaron behavior: instead of the strong P_1 and P_2 bands of polarons, F_2^{-2} and F_3^{-2} dianions each possess a single strong band between the P_1 and P_2 bands of the anions, with an additional weak band at higher energy. Dianions of long oligomers are different. Figure 12 compares spectra from Figure 4 for F_{10}^{-2} with the anions $F_5^{-\bullet}$ and $F_{10}^{-\bullet}$. This comparison makes it clear that strong P_1 and P_2 bands of anions $F_5^{-\bullet}$ and $F_{10}^{-\bullet}$ are very similar. In the P_1 and P_2 region the spectrum of F_{10}^{-2} is also similar, but twice as intense. Figure 12

dx.doi.org/10.1021/ja301494n | J. Am. Chem. Soc. 2012, 134, 10852−10863

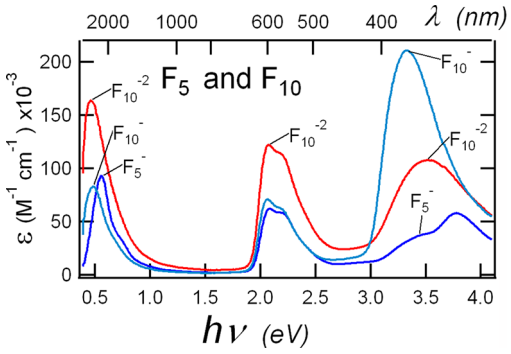

Figure 12. Comparison of the absorption spectra of F_5 and F_{10} anions and the F_{10} dianion. P_1 at 0.5 eV, P_2 at 2.2 eV, and VN at 3.2−3.8 eV.

clearly supports the idea that F_{10}^{-2} is two polarons nearly identical to the single polaron in $F_{10}^{-\bullet}$ It is also notable that the VN band of $F_{10}^{-\bullet}$ is larger than its P_1 and P_2 bands, the VN band of F_{10}^{-2} is smaller, and that of $F_5^{-\bullet}$ is still smaller. These observations are in complete accord with the conclusion that F_{10}^{-2} contains two side-by-side polarons, doubling the intensities of both the P_1 and P_2 bands, while occupying most of the chain to give a weak VN band. Figure 12 also shows that the P_1 band of $F_5^{-\bullet}$ is sharper than the P_1 bands in the F_{10} ions. This broadening is the subject of the next section.

With increasing oligomer length the evolution from bipolaron in F_4^{-2} to two side-by-side polarons in F_6^{-2} is evident. The criterion that bipolarons would have single transitions suggests that F_4^{-2} is principally a bipolaron, F_6^{-2} is principally a pair of polarons, and F_5^{-2} is intermediate. The gradual evolution, rather than an abrupt change, is consistent with a picture in which bipolaronic and two-polaron configurations are mixed with a decreasing bipolaron fraction in F_4^{-2}–F_6^{-2}. The fact that no dianion exhibits a spectrum that is the sum of a two-band (polarons) and single-band (bipolarons) also reflects this gradual evolution, passing through states of mixed character. Such a gradual evolution is required by computed orbitals (Figure 8) and the evolution of $\langle S^2 \rangle$, but the computed results suggest that the evolution from bipolarons to two polarons occurs closer to F_3^{-2}, possibly due to the absence of counterions.

Broadening of Spectra in Long Oligomers. Optical spectra of anions from naphthalene through pentacene display progressively sharper bands as the length of the molecule increases.[62] This may be because delocalized ions of large molecules interact less strongly with their environment as expressed in the Born equation[63] for solvation. For the present data, shown in Figure 4, bands of $F_3^{-\bullet}$ are sharper than those of $F_2^{-\bullet}$, but then the trend reverses. The P_1 bands of $F_{10}^{-\bullet}$ and all long oligomers are broader than those of $F_5^{-\bullet}$. The contrast with the well-resolved spectrum of $F_3^{-\bullet}$ is even greater, as seen in Figure 5. The transition from sharp to broadened spectra occurs at the 4.5 ± 0.5 unit delocalization length of the polaron, suggesting the following conclusion: Polarons confined by the length of the oligomers yield sharp spectra, while spectra for unconfined polarons in long oligomers or polymers are broadened.

Unconfined polarons, those residing in oligomers longer than the polaron length, may not have a single length. Instead thermal energy can cause fluctuations of dihedral angles. Smaller dihedral angles can lengthen the polaron as depicted in Figure 10 d, so its length, and therefore the energy of its transitions, may fluctuate, producing broadening. Unconfined polarons are therefore dynamic objects with fluctuating lengths. To check this proposal uωB97XD optimized structures for $F_3^{-\bullet}$, having a confined polaron, and $F_{10}^{-\bullet}$, having an unconfined polaron, were "flattened": all dihedral angles were set to zero. TD calculations (uωB97XD/3-21 g) on the flattened structures gave P_1 transition energies that were almost unchanged (+3%) for $F_3^{-\bullet}$, but decreased by 32% for $F_{10}^{-\bullet}$. These computed results confirm the idea that dihedral angles regulate the energy of the P_1 transition in long, but not in short oligomers, supporting this mechanism of spectral broadening in anions of long oligomers.

SYNOPSIS AND CONCLUSIONS

Absorption spectra of anions and dianions of F_1–F_{10} oligofluorenes were produced using Na, NaBip, and NaK. Accurate reduction potentials were obtained from equilibria. Optical spectra of the singly reduced oligomers exhibit the following behavior: (1) They contain the NIR P_1 bands and visible P_2 bands typical of polarons. (2) The P_1 bands, and to a lesser extent the P_2 bands, shifted to lower energy with increasing oligomer length, n, but leveled out for $n > 5$, suggesting a polaron length of $\lesssim$5. (3) The dependence of the transition energy, $E(P_1)$ was reproduced well by TD-DFT calculations using long-range-corrected functionals but not with traditional functionals such as B3LYP. The long-range-corrected functionals also compute orbitals that accommodate the added electron (SOMOs) having lengths of ∼4 repeat units. (4) For $n > 5$ the bands became broader, which can be explained by fluctuations in the length of the polarons. (5) Addition of the electron removed the strong absorption band of F_2 and F_3 neutrals, but for $n \geq 4$ vestigial neutral (VN) bands remained. E_{max} for the VN band of $F_{10}^{-\bullet}$ was slightly blue-shifted relative to the band of F_{10} neutral. This blue-shift became larger for shorter oligomers. Sometimes at 1.0 electron/molecule two bands were resolvable in the neutral region: shifted VN bands of $F_n^{-\bullet}$ and unshifted bands from disproportionation. Positions, E_{max}, of the VN bands of $F_n^{-\bullet}$ are similar to those of F_n that are 4.0 units shorter. With the assumption that negative polarons and neutrals occupy strictly separate regions, VN bands estimate the length of the polaron to be 4.0 repeat units. Taking into account anion transition energies, broadening of anion bands, VN bands in anions, and behaviors of dianions lead to n_{deloc} = 4.3 ± 0.5. Excitons in neutral F_n oligomers similarly appear to be polarons having lengths of 5 ± 1 repeat units.

Dianions, F_n^{-2}, show classic bipolaron spectra with a single band for F_2^{-2} and F_3^{-2}, but conform to the picture of two side-by-side polarons for $n \gtrsim 7$. At intermediate lengths the dianions gradually shift between these two paradigms. VN bands are present in spectra of F_n^{-2} for $n \gtrsim 7$, but they are much less intense and more blue-shifted than those of the corresponding anions. DFT computations with long-range-corrected functionals are compatible with the experiments. In long oligomers ($n \gtrsim 4$) the computations find the two added electrons to occupy two separate, side-by-side orbitals, and unrestricted singlet Kohn–Sham calculations give $\langle S^2 \rangle$ near 1.0. For short oligomers the two added electrons occupy nearly identical spatial orbitals and $\langle S^2 \rangle \sim 0$. The computations also suggest a gradual shift from bipolarons to two polarons. While the measures of $\langle S^2 \rangle$ and the spatial extents of the orbitals suggest that the shift occurs at a shorter length than suggested by the changes in the optical spectra, neither measure is precise. An

dx.doi.org/10.1021/ja301494n | J. Am. Chem. Soc. 2012, 134, 10852–10863

important conclusion is that both the experiments and computations support the formation at mixed states at intermediate lengths. These mixed states have character intermediate between that of bipolarons and two-polarons.

These behaviors are consistent with the following picture: A single charge is a polaron having a length of 4.3 ± 0.5 repeat units (3.6 nm). Two charges in a single conjugated chain of length ∼8 or more repeat units are more stable as two separate polarons. In short chains the repulsion and compression of two polarons is sufficiently large that a bipolaron is more stable. The two states may blend at intermediate lengths. A subtlety suggested by the VN bands is that two polarons in one chain may occupy slightly less space (length) than the sum of lengths of two completely separate polarons.

EXPERIMENTAL SECTION

Chemicals. Synthesis of F_1−F_{10} oligofluorenes by the method of Klearner[64] has been described.[65] Tetrahydrofuran (THF) was purified by distillation from Na/benzophenone. 1,4-Dicyanobenzene (DCNB) and the 2.2.2 Cryptand (C222) were used as received from Aldrich.

Spectroscopy. Ultraviolet−visible−near-infrared (UV−vis−NIR) absorption spectroscopy was performed at room temperature from 200 to 3200 nm on a Cary 5 spectrometer (Varian Instruments) using 1 mm path length dry quartz spectrophotometric cells. Extinction coefficients for F_1−F_{10} neutrals were calculated from the slopes of the absorbance (A) versus concentration curves of calibration standards using the Beer−Lambert Law, $A = \varepsilon cl$. Extinction coefficients for each anionic species were determined from the maximum absorbance for the spectrum that corresponded to 100% of that species based upon the starting concentration of neutral F_n. Fluorescence emission spectra were obtained on a Horiba Jobin Yvon Fluoromax 4 with 1 cm path length dry quartz cells on F_1−F_{10} samples with a 2×10^6 M concentration in THF. The excitation wavelength was 265 nm for F_1, and 300 nm for F_2−F_{10}. Data were processed using IGOR Pro (Wavemetrics).

Chemical Reductions with Sodium. A glass apparatus was fabricated to run the sodium metal reduction reactions in timed intervals under vacuum conditions.[66] The apparatus has a dry quartz spectrophotometric cell, a 10 mL round-bottom flask, a vacuum attachment, and a side arm with constrictions to facilitate purification of sodium by successive vacuum sublimations at 10^{-4} Torr with a torch. Five milliliters of purified THF was distilled from sodium and benzophenone into the round-bottom flask, and the apparatus was rotated to transfer THF to the quartz cell containing solid F_n. F_n concentrations were varied from 20 to 200 μM to obtain appropriately scaled absorbances. Electrons were transferred to each F_n sample by rotating the apparatus to contact the F_n solution with the sodium mirror in timed intervals. Electron transfers were monitored by UV−vis−NIR spectroscopy. Because this method could not accurately determine the number of reducing equivalents added, two others were employed. Use of two or three methods in some cases provided additional certainty.

Chemical Reductions with Sodium Potassium Alloy and Titrations with DCNB. F_n oligofluorenes were reacted with sodium potassium (NaK) alloy under an inert argon atmosphere at room temperature and transferred to a glass apparatus for titrations with acceptors such as 1,4-dicyanobenzene (DCNB) to confirm the spectral identity of each reduced species.

Chemical Reductions with Sodium Biphenyl. Titrations were performed under an inert argon atmosphere in an apparatus fitted with a syringe and round-bottom flask attached to a 1 mm path length dry quartz optical cell. Commercial sodium biphenyl, ∼1 M in 1,2-dimethoxyethane (GFS Chemicals), was diluted by a factor of 8 with dimethoxyethane. Diluted sodium biphenyl was added by 100 μL syringe to 5 mL of purified and dried tetrahydrofuran (THF) to remove traces of residual water, as evidenced by the change from colorless to light blue. Oligofluorenes were weighed and dissolved in 5 mL of the dry THF. Concentrations were 100−200 μM for F_2−F_5 and 30−100 μM for F_6−F_{10}. Solutions were titrated with sodium biphenyl in 1.0, 2.5, or 5.0 μL increments, and UV−vis−NIR spectra were recorded after each addition. The biphenyl anion concentration was calibrated for each experiment utilizing the known extinction coefficients 40,000 (400 nm) and 12,500 (630 nm).[67] The number of reducing equivalents was not perfectly reproducible, probably due to slow leaching of water from the glassware even though it was oven-dried. Especially from the longer oligomers this made the determination of electrons added per molecule uncertain by as much as 0.3 equiv in some cases. Measurements of molar extinction coefficients at LEAF enabled a calibration accurate to 0.07 equiv. For short oligomers (n = 2−4) the spectra for addition of 1, 2, and 3 electrons were distinct, making the points at which n = 1.0 or 2.0 equiv unambiguous, even if the equivalents added were uncertain. For these, accurate extinction coefficients could be determined directly from the titrations.

Pulse Radiolysis. Experiments to determine the extinction coefficients of the F_3−F_{10} anions were performed at the Laser-Electron Accelerator Facility (LEAF) at Brookhaven National Laboratory.[68] Solutions were prepared in 1.2 mL of THF at the concentrations of 100−200 μM both without and with addition of tetrabutylammoniumhexylfluorophosphate. Pulse radiolysis with <50 ps electron pulses was performed as described previously.[36,59] Biphenyl and benzophenone (300 μM in 1.2 mL THF) were used as reference samples with known extinction coefficients.[67,69]

Computations. were carried out with *Gaussian03*[70] and *Gaussian09*[71] and *Q-Chem*[72] programs using different exchange-correlation approximations in density functional theory (DFT). All hexyl groups are replaced by H atoms. For each system, be it neutral or charged, the geometry is fully optimized without symmetry constraints. Linear response time-dependent (TDDFT) calculations are then performed for low-lying excited states. Calculations in vacuum with ωPBE[54] were done with *Q-Chem*,[73] and those with the PCM solvation model[74−76] were done in *Gaussian09*,[71] while those of ωB97X-D[50] were done with *Gaussian03*. Most calculations used the 6-31G* basis set and the PCM solvation model.[74−76] All calculations on anions and dianions were unrestricted.

ASSOCIATED CONTENT

Supporting Information

Graphs comparing all anions and dianions, transient bleaching spectra, table of vibrational spacings, and part of a titration and full author lists for refs 70, 71, and 72. Coordinates and energies from ωPBE optimizations for anions used to compute points that successfully described the experimental results in Figure 6 and coordinates and energies for anions and dianions depicted in Figures 7 and 8. This material is available free of charge via the Internet at http://pubs.acs.org.

AUTHOR INFORMATION

Corresponding Author

jrmiller@bnl.gov

Present Address

[⊥]Department of Biomolecular Engineering, Kyoto Institute of Technology, Matsugasaki, Sakyo-ku, Kyoto 606-8585, Japan

Notes

The authors declare no competing financial interest.

ACKNOWLEDGMENTS

We gratefully acknowledge support of the Division of Chemical Sciences, Geosciences, and Biosciences, Office of Basic Energy Sciences of the U.S. Department of Energy through Grant #DE-AC02-98-CH10886 to all authors, and for use of the LEAF Facility of the BNL Accelerator Center for Energy Research. L.Z. and E.S. thank the National Science Foundation Awards #03-35799 and #09-34814 for support of their work in

the FaST Program at BNL. C.G., A.Y. and J.R. thank the High School Research Program at BNL. L.Z. and P.K. acknowledge support from Dowling College. We are grateful to Stefano Quarta for some preliminary spectra. Some of the computations were carried out at the Center for Functional Nanomaterials, Brookhaven National Laboratory, which is supported by the U.S. Department of Energy, Office of Basic Enregy Science, under Contract #DE-AC02-98CH10886.

REFERENCES

(1) Heeger A. J., MacDiarmidA. G., Shirakawa H. *The Nobel Prize in Chemistry*; 2000, http://www.nobelprize.org/nobel_prizes/chemistry/laureates/2000/.
(2) Fichou, D.; Horowitz, G.; Garnier, F. *Synth. Met.* **1990**, *39*, 125−131.
(3) Fichou, D.; Horowitz, G.; Xu, B.; Garnier, F. *Synth. Met.* **1990**, *39*, 243−259.
(4) Hotta, S.; Waragai, K. *J. Mater. Chem.* **1991**, *1*, 835−842.
(5) Guay, J.; Kasai, P.; Diaz, A.; Wu, R. L.; Tour, J. M.; Dao, L. H. *Chem. Mater.* **1992**, *4*, 1097−1105.
(6) Hill, M. G.; Penneau, J. F.; Zinger, B.; Mann, K. R.; Miller, L. L. *Chem. Mater.* **1992**, *4*, 1106−1113.
(7) Zinger, B.; Mann, K. R.; Hill, M. G.; Miller, L. L. *Chem. Mater.* **1992**, *4*, 1113−1118.
(8) Zotti, G.; Martina, S.; Wegner, G.; Schluter, A. D. *Adv. Mater.* **1992**, *4*, 798−801.
(9) Bauerle, P.; Segelbacher, U.; Maier, A.; Mehring, M. *J. Am. Chem. Soc.* **1993**, *115*, 10217−10223.
(10) Hotta, S.; Waragai, K. *J. Phys. Chem.* **1993**, *97*, 7427−7434.
(11) Khanna, R. K.; Jiang, Y. M.; Srinivas, B.; Smithhart, C. B.; Wertz, D. L. *Chem. Mater.* **1993**, *5*, 1792−1798.
(12) Horowitz, G.; Yassar, A.; Vonbardeleben, H. J. *Synth. Met.* **1994**, *62*, 245−252.
(13) Zade, S. S.; Zamoshchik, N.; Bendikov, M. *Acc. Chem. Res.* **2011**, *44*, 14−24.
(14) van Haare, J.; Havinga, E. E.; van Dongen, J. L. J.; Janssen, R. A. J.; Cornil, J.; Bredas, J. L. *Chem.—Eur. J.* **1998**, *4*, 1509−1522.
(15) Chi, C. Y.; Im, C.; Wegner, G. *J. Chem. Phys.* **2006**, *124*, 8.
(16) Chi, C. Y.; Wegner, G. *Macromol. Rapid Commun.* **2005**, *26*, 1532−1537.
(17) Fratiloiu, S.; Grozerna, F. C.; Koizumi, Y.; Seki, S.; Saeki, A.; Tagawa, S.; Dudek, S. P.; Siebbeles, L. D. A. *J. Phys. Chem. B* **2006**, *110*, 5984−5993.
(18) Fesser, K.; Bishop, A. R.; Campbell, D. K. *Phys. Rev. B* **1983**, *27*, 4804−4825.
(19) Harbeke, G.; Baeriswyl, D.; Kiess, H.; Kobel, W. *Phys. Scr.* **1986**, *T13*, 302−305.
(20) Bredas, J. L.; Street, G. B. *Acc. Chem. Res.* **1985**, *18*, 309−315.
(21) Zade, S. S.; Bendikov, M. *J. Phys. Chem. B* **2006**, *110*, 15839−15846.
(22) Jansson, E.; Jha, P. C.; Aren, H. *Chem. Phys.* **2007**, *336*, 91−98.
(23) Cornil, J.; Beljonne, D.; Bredas, J. L. *J. Chem. Phys.* **1995**, *103*, 842−849.
(24) Kaneto, K.; Hayashi, S.; Ura, S.; Yoshino, K. *J. Phys. Soc. Jpn.* **1985**, *54*, 1146−1153.
(25) Furukawa, Y. *J. Phys. Chem.* **1996**, *100*, 15644−15653.
(26) Sworakowski, J.; Ulanski, J. *Annu. Rep. Sect. C (Phys. Chem.)* **2003**, *99*, 87−125.
(27) Goh, C.; McGehee, M. D. *Bridge, Natl. Acad. Eng.* **2005**, *35*, 33−9.
(28) Goldsmith, R. H.; Sinks, L. E.; Kelley, R. F.; Betzen, L. J.; Liu, W. H.; Weiss, E. A.; Ratner, M. A.; Wasielewski, M. R. *Proc. Natl. Acad. Sci. U.S.A.* **2005**, *102*, 3540−3545.
(29) Miura, T.; Carmieli, R.; Wasielewski, M. R. *J. Phys. Chem. A* **2010**, *114*, 5769−5778.
(30) Wielopolski, M.; Santos, J.; Illescas, B. M.; Ortiz, A.; Insuasty, B.; Bauer, T.; Clark, T.; Guldi, D. M.; Martin, N. *Energy Environ. Sci.* **2011**, *4*, 765−771.
(31) Atienza-Castellanos, C.; Wielopolski, M.; Guldi, D. M.; van der Pol, C.; Bryce, M. R.; Filippone, S.; Martin, N. *Chem. Commun.* **2007**, 5164−5166.
(32) van der Pol, C.; Bryce, M. R.; Wielopolski, M.; Atienza-Castellanos, C.; Guldi, D. M.; Filippone, S.; Martin, N. *J. Org. Chem.* **2007**, *72*, 6662−6671.
(33) Shibano, Y.; Imahori, H.; Sreearunothai, P.; Cook, A. R.; Miller, J. R. *J. Phys. Chem. Lett.* **2010**, *1*, 1492−1496.
(34) Burrows, H. D.; de Melo, J. S.; Forster, M.; Guntner, R.; Scherf, U.; Monkman, A. P.; Navaratnam, S. *Chem. Phys. Lett.* **2004**, *385*, 105−110.
(35) Grozema, F. C.; Warman, J. M. *Radiat. Phys. Chem.* **2005**, *74*, 234−238.
(36) Asaoka, S.; Takeda, N.; Lyoda, T.; Cook, A. R.; Miller, J. R. *J. Am. Chem. Soc.* **2008**, *130*, 11912−11920.
(37) Albuquerque, R. Q.; Hofmann, C. C.; Kohler, J.; Kohler, A. *J. Phys. Chem. B* **2011**, *115*, 8063−8070.
(38) Chen, L. Y.; Hung, W. Y.; Lin, Y. T.; Wu, C. C.; Chao, T. C.; Hung, T. H.; Wong, K. T. *Appl. Phys. Lett.* **2005**, 87.
(39) DeLongchamp, D. M.; Ling, M. M.; Jung, Y.; Fischer, D. A.; Roberts, M. E.; Lin, E. K.; Bao, Z. N. *J. Am. Chem. Soc.* **2006**, *128*, 16579−16586.
(40) Herrnsdorf, J.; Guilhabert, B.; Chen, Y.; Kanibolotsky, A. L.; Mackintosh, A. R.; Pethrick, R. A.; Skabara, P. J.; Gu, E.; Laurand, N.; Dawson, M. D. *Opt. Express* **2010**, *18*, 25535−25545.
(41) Wallace, J. U.; Chen, S. H. In *Polyfluorenes*; Scherf, U., Neher, D., Eds.; Springer-Verlag: Berlin, 2008; Vol. *212*, pp 145−186.
(42) Wang, Y.; Tsiminis, G.; Yang, Y.; Ruseckas, A.; Kanibolotsky, A. L.; Perepichka, I. F.; Skabara, P. J.; Turnbull, G. A.; Samuel, I. D. W. *Synth. Met.* **2010**, *160*, 1397−1400.
(43) Wei, S. K. H.; Chen, S. H.; Dolgaleva, K.; Lukishova, S. G.; Boyd, R. W. *Appl. Phys. Lett.* **2009**, 94.
(44) Cohen, A. J.; Mori-Sanchez, P.; Yang, W. T. *Science* **2008**, *321*, 792−794.
(45) Perdew, J. P.; Zunger, A. *Phys. Rev. B* **1981**, *23*, 5048−5079.
(46) Zhang, Y. K.; Yang, W. T. *J. Chem. Phys.* **1998**, *109*, 2604−2608.
(47) Iikura, H.; Tsuneda, T.; Yanai, T.; Hirao, K. *J. Chem. Phys.* **2001**, *115*, 3540−3544.
(48) Perdew, J. P.; Burke, K.; Ernzerhof, M. *Phys. Rev. Lett.* **1996**, *77*, 3865−3868.
(49) Yanai, T.; Tew, D. P.; Handy, N. C. *Chem. Phys. Lett.* **2004**, *393*, 51−57.
(50) Chai, J. D.; Head-Gordon, M. *Phys. Chem. Chem. Phys.* **2008**, *10*, 6615−6620.
(51) Jo, J. H.; Chi, C. Y.; Hoger, S.; Wegner, G.; Yoon, D. Y. *Chem.—Eur. J.* **2004**, *10*, 2681−2688.
(52) Slates, R. V.; Szwarc, M. *J. Phys. Chem.* **1965**, *69*, 4124−4131.
(53) Funston, A. M.; Silverman, E. E.; Miller, J. R.; Schanze, K. S. *J. Phys. Chem. B* **2004**, *108*, 1544−1555.
(54) Henderson, T. M.; Janesko, B. G.; Scuseria, G. E. *J. Chem. Phys.* **2008**, *128*, 194105.
(55) Zamoshchik, N.; Bendikov, M. *Adv. Funct. Mater.* **2008**, *18*, 3377−3385.
(56) Szabo, A.; Ostlund, N. S. *Modern Quantum Chemistry: Introduction to Advanced Electronic Structure Theory*; Dover: New York, 1996.
(57) Borden, W. T.; Davidson, E. R. *J. Am. Chem. Soc.* **1977**, *99*, 4587−4594.
(58) Gao, Y.; Liu, C. G.; Jiang, Y. S. *J. Phys. Chem. A* **2002**, *106*, 5380−5384.
(59) Takeda, N.; Asaoka, S.; Miller, J. R. *J. Am. Chem. Soc.* **2006**, *128*, 16073−16082.
(60) Shalev, H.; Evans, D. H. *J. Am. Chem. Soc.* **1989**, *111*, 2667−2674.
(61) Streitweiser, A. J.; Schwager, I. *J. Phys. Chem.* **1962**, *66*, 2316.
(62) Buschow, K. H. J.; Hoijtink, G. J. *J. Chem. Phys.* **1964**, *40*, 2501−04.
(63) Born, M. *Z. Phys.* **1920**, *1*, 45−8.
(64) Klaerner, G.; Miller, R. D. *Macromolecules* **1998**, *31*, 2007−2009.

(65) Sreearunothai, P.; Asaoka, S.; Cook, A. R.; Miller, J. R. *J. Phys. Chem. A* **2009**, *113*, 2786−2795.
(66) Petrov, E. S.; Terekhova, M. I.; Shatenshtein, A. I. *Russ. Chem. Rev.* **1973**, *42*, 713−24.
(67) Jagur-Grodzinski, J.; Feld, M.; Yang, S. L.; Szwarc, M. *J. Phys. Chem.* **1965**, *69*, 628−35.
(68) Wishart, J. F.; Cook, A. R.; Miller, J. R. *Rev. Sci. Instrum.* **2004**, *75*, 4359−4366.
(69) Pedersen, S. U.; Christensen, T. B.; Thomasen, T.; Daasbjerg, K. *J. Electroanal. Chem.* **1998**, *454*, 123−143.
(70) Frisch, M. J.; et al. *Gaussian03*, A.1 ed.; Gaussian Inc.: Pittsburgh, PA, 2003.
(71) Frisch, M. J.; et al. *Gaussian09*, A.1 ed.; Gaussian Inc.: Wallingford, CT, 2009.
(72) Shao, Y.; et al. *Phys. Chem. Chem. Phys.* **2006**, *8*, 3172−3191.
(73) Rohrdanz, M. A.; Herbert, J. M. *J. Chem. Phys.* **2008**, 129.
(74) Tomasi, J.; Mennucci, B.; Cammi, R. *Chem. Rev.* **2005**, *105*, 2999−3093.
(75) Improta, R.; Scalmani, G.; Frisch, M. J.; Barone, V. *J. Chem. Phys.* **2007**, 127.
(76) Improta, R.; Barone, V.; Scalmani, G.; Frisch, M. J. *J. Chem. Phys.* **2006**, 125.